Available online at www.sciencedirect.com
SCIENCE DIRECT®
Materials Chemistry and Physics 92 (2005) 295–302
MATERIALS CHEMISTRY AND PHYSICS
www.elsevier.com/locate/matchemphys

Electrical and sintering behaviour of $Y_2Zr_2O_7$ (YZ) pyrochlore-based materials—the influence of bismuth

M. Kumar, M. Anbu Kulandainathan, I. Arul Raj, R. Chandrasekaran, R. Pattabiraman *

Central Electrochemical Research Institute, Karaikudi 630006, India

Received 13 January 2004; accepted 14 May 2004

Abstract

Solid oxide fuel cell can convert fuels rich in H_2 into electrical energy directly without pollution by electrochemical reaction with oxygen. The efficiency of energy conversion and durability of performance mainly depend on the oxide ion conducting solid electrolyte activity. The global experience gained all these years in the solid oxide fuel cell (SOFC) development has prompted for a change from the state of the art functional electrolyte material, yttria-stabilized zirconia (YSZ), having a conductivity of 0.1 S cm^{-1} at 1000 °C, to a new material which exhibits equivalent conductivity values in the intermediate temperature range (600–700 °C). In this work, yttrium zirconate ($Y_2Zr_2O_7$ (YZ)), an ionic conducting stable pyrochlore-based oxide prepared by glycine nitrate combustion route, is systematically characterised. Both circular and rectangular pellets were fabricated by uniaxial compression followed by annealing at different temperatures. The functional properties such as porosity, percentage thermal shrinkage in volume and percentage densification of the sintered pellets are compiled. Bismuth oxide is found to be an effective sintering aid in general. So, the effect of bismuth oxide addition on YZ was investigated through sintering studies, X-ray diffraction (XRD), TGA/DTA, scanning electron microscopy (SEM) and conductivity measurements. The results obtained on YZ with and without bismuth oxide addition are discussed with respect to the requirement of an electrolyte for intermediate temperature solid oxide fuel cell (ITSOFC) application.

Keywords: Electrolyte; Intermediate temperature solid oxide fuel cells; Electrical and sintering study

1. Introduction

Fuel cells are electrochemical devices, which offer direct conversion of a variety of fuels into electrical power. Several types of fuel cells are under development owing to their environmental compatibility, potential for use in stationary and distributed electric power stations, as well as in transportation applications. They are solid polymer electrolyte fuel cells (SPEFC), alkaline fuel cell (AFC), direct methanol fuel cell (DMFC), phosphoric acid fuel ceil (PAFC), molten carbonate fuel cells (MCFC) and solid oxide fuel cell (SOFC). Among these systems, SOFC has striking features, namely, high-energy conversion efficiency, use of non-precious materials, no liquids are involved and adaptation to variety of fuels and invariant electrolyte [1–3]. The high-temperature operation of SOFC causes many serious problems such as severe restriction on the choice of materials, electrode sintering programme, interfacial diffusion across the electrolyte and electrodes and mechanical stresses due to difference in their thermal expansion/shrinkage value. The thermal compatibility of the LSM cathode–yttria-stabilized zirconia (YSZ) interface is not adequate enough on prolonged operation in SOFC, resulting in the formation of insulating phases across the interface leading to performance degradation due to rise in the cell resistance with time [4]. In order to overcome these problems, the researchers have introduced the reduced/intermediate temperature solid oxide fuel cell (ITSOFC) operating at 600–800 °C are developed. Two approaches are considered in ITSOFC research.

* Corresponding author. Tel.: +91 4565 42 7550x559; fax: +91 4565 42 7713.
E-mail address: rpraman_insaest@yahoo.com (R. Pattabiraman).

0254-0584/$ – see front matter © 2004 Published by Elsevier B.V.
doi:10.1016/j.matchemphys.2004.05.050

1. use of this electrolyte membrane to make the ohmic loss due to electrolyte as minimum as possible.
2. to identify new electrolyte materials, which exhibit high oxide ion conductivity at reduced temperature.

Attempts to replace YSZ by rare earth pyrochlores exhibiting high ion conductivity have been reported [5–12]. In this paper, we have discussed on the synthesis, characterisation and sintering of the yttrium zirconate ($Y_2Zr_2O_7$ (YZ)) parent pyrochlore. The effect of bismuth on the physical properties and sintering behaviour of YZ pyrochlore-based materials is brought out.

2. Experimental

2.1. Powder preparation

High-purity yttrium oxide, zirconyl nitrate and glycine were used as the starting materials. The stoichiometric compositions of mixtures for the combustion were calculated using the total oxidising (O) and reducing (F) valencies of the components, which serve as a numerical coefficient for the stoichiometric balance, so that the oxidant to the fuel ratio is 1:2.78 for the yttrium zirconate synthesis. The yttrium zirconate was obtained by glycine–nitrate synthesis route, which involved rapid heating of an aqueous concentrated solution containing respective starting materials at 550 °C [13]. The solution initially boiled, underwent rapid degradation and foaming followed by decomposition, generating gases such as CO_2, N_2, H_2O. The gases ignited and burnt with temperature above 1000 °C, yielding voluminous oxide. The obtained oxide was calcined at 800 °C for 3 h to remove the unburnt materials and to obtain the most stable mixed oxide phases.

2.2. Sample preparation and characterisation

The combustion-derived pyrochlore powder was characterised by powder X-ray diffraction (XRD), density, particle size, FTIR and TGA/DTA. The XRD patterns were obtained with a diffractometer (JEOL-8030 X-ray diffractometer) using Cu Kα radiation. The density of the calcined pyrochlore powders was measured using pycnometer with xylene as the liquid medium. Horiba laser particle size analyser (LA-910) was used to determine the particle size distribution of calcined yttrium zirconate pyrochlores. Fourier transform infrared spectra of yttrium zirconate pyrochlores was recorded using a Perkin-Elmer paragon 500 model FTIR spectrometer as KBr pellets. The thermal characterisation of the precalcined powder was carried out by PL Thermal Sciences unit at a heating rate of 10 °C min^{-1} in static air.

The combustion-derived YZ powder and powder YZ with various weight percent of bismuth oxide addition were mixed and crushed in an agate mortar and pelletized by applying 5-ton load. These pellets were subjected to sintering at various temperatures ranging from 900 to 1200 °C for 0, 2.5, 5.0 and 7.5% bismuth oxide addition, and the YZ pellets containing 5, 10, 15 and 20% bismuth oxide were subjected to sintering at constant temperature, 1200 °C, for studying the effect of bismuth oxide addition at 1200 °C at 3 h dwell time. From the data obtained, the sintering behaviour and the porosity of these pellets were measured by liquid adsorption technique using dioxan as a medium. The conductivity measurements on YZ with and without bismuth oxide pellets were carried out in air using a.c. impedance spectroscopy in the frequency ranging from 100 Hz to 100 kHz. The microstructure analysis of these pellets was studied using scanning electron microscopy (SEM).

3. Results and discussions

The XRD pattern of the parent yttrium zirconate is shown in Fig. 1. The *D*-values obtained are in agreement with the formation of pyrochlore phase as reported [13] in literature. No new phase is found even for the sample with 5% bismuth oxide addition. However, the JCPDS data files corresponding to the pyrochlore oxides are not available for comparison.

By using Scherrer equation, the average crystallite size of yttrium zirconate pyrochlore materials is calculated from the broadening of a specific diffraction peak. The equation used is

$$D = \frac{0.9\lambda}{\beta \cos \theta}$$

where D is the average size of the crystallites, 0.9 is the Scherrer constant, λ is wave length of radiation, β is the peak width at half-height and θ corresponds to the peak position. The crystallite size of YZ is 3.782 nm. It reveals that the

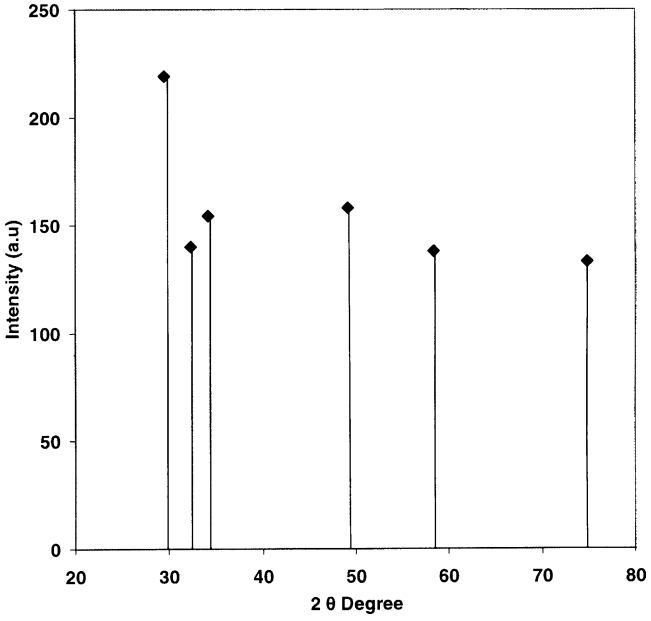

Fig. 1. XRD pattern for yttrium zirconate powder.

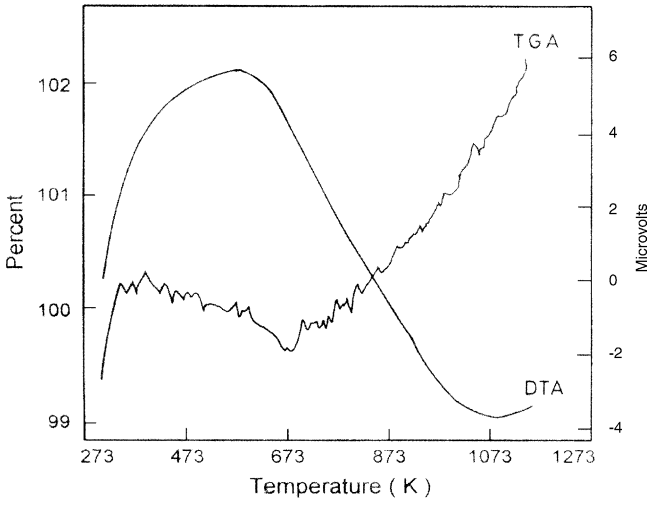

Fig. 2. Thermal analysis and differential thermal analysis of yttrium zirconate with 20 weight percent of bismuth oxide.

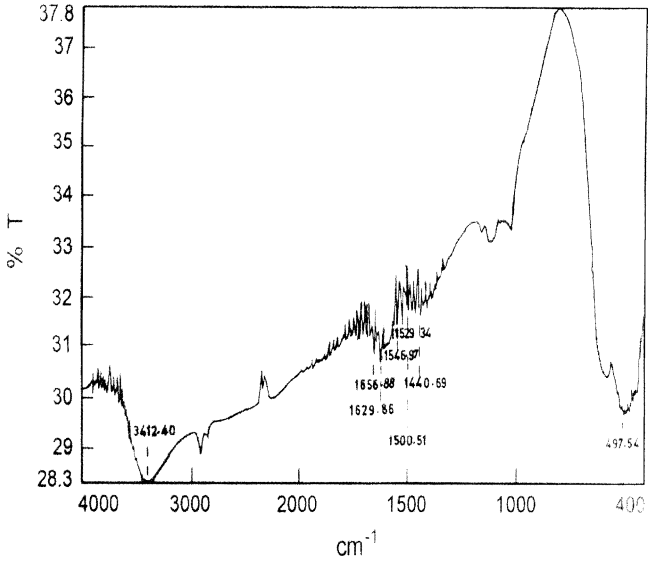

Fig. 3. Fourier transform infrared spectroscopy for yttrium zirconate.

densification of the YZ pyrochlore compound at high temperature is less. Because of smaller crystallite size, the material has larger surface-free energy [14]. Generally, the reduction of surface-free energy is the driving force for sintering of the material [15], which is the reason for the low densification of YZ at high temperature. Hence, in order to sinter the YZ materials well even at low temperature, it was felt necessary to add bismuth oxide with various weight percent as sintering aid.

The TG and the DTA patterns obtained on YZ with bismuth oxide addition are shown in Fig. 2. A gain in the weight occurred initially and then a gradual loss occurred up to 400 °C, which was followed by weight gain up to 900 °C. The DTA curve shows broad exothermic peak at 320 °C, which is due to evolution of gases as observed in the TG curve. The DTA curve for YZ with bismuth oxide did not show any sharp endothermic peak, which from due to melting of bismuth oxide, at 824 °C, the melting point of bismuth oxide. The TG and DTA analysis did not show a weight loss in TG and endothermic peak in DTA in the temperature range between 600 and 900 °C. It reveals that there is no indication for removal of leaving any extra oxygen from the lattice [16].

The FTIR spectra obtained on pyrochlore materials are shown in Fig. 3. It shows that the peak observed at 500 cm^{-1} corresponds to the pyrochlore phase, which is in good agreement with the literature data [13].

The particle size distribution of YZ is shown in Fig. 4. It is evident that 60% of the particles in the bulk are below 7.3 μm in size. The bulk, tap and absolute densities of YZ powder with and without bismuth oxide addition are presented in Table 1.

The effect of bismuth oxide addition on the densification behaviour of the representative compositions $Y_2Zr_2O_7$ with respect to temperature is clearly evident from Fig. 5 in which percent theoretical density is plotted against the sintering temperature. For all the samples, the extent of sintering is negligible below 800 °C. For YZ without bismuth oxide, the densification increases very slowly with increasing temperature. A maximum of around 40% densification occurs at a sintering temperature of 1200 °C. But there is sudden increase in density at 1200 °C for yttrium zirconate with bismuth oxide addition of 2.5, 5.0 and 7.5 wt.%.

For enhancing the sintering rate at a fixed temperature, the effect of various weight percent of bismuth oxide addition (i.e., 5, 10, 15 and 20%) has been studied. The obtained percent theoretical density is plotted against various percent of bismuth oxide and shown in Fig. 6. From the graph, it is found that the YZ without bismuth oxide densify only to 40% at 1200 °C, but the percentage of densification increases with increase in the bismuth oxide content in YZ. This result clearly shows the effectiveness of bismuth oxide as sintering aid for the material YZ.

The porosity values of the yttrium zirconate with and without bismuth oxide were measured by liquid adsorption

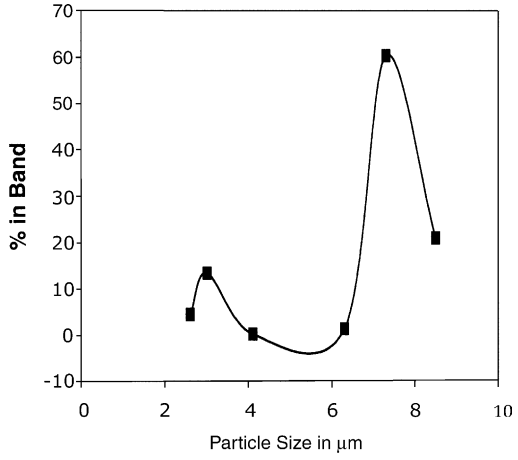

Fig. 4. The particle size distribution of yttrium zirconate powder.

Table 1
Physical properties of yttrium zirconate with and without bismuth oxide

wt.%Bi_2O_3	Powder density (g cc^{-1})			Percentage theoretical density of pellets sintered at 1200 °C	$\sigma \times 10^{-3}$ S cm^{-1} at 500 °C	$\sigma \times 10^{-3}$ S cm^{-1} at 800 °C	Energy of activation (kJ)
	Bulk density	Tap density	Absolute density				
0	0.165	0.3056	2.403	40.14	1.770	3.750	7.841
5	0.161	0.250	1.950	64.94	2.046	0.460	−15.423
10	0.177	0.274	4.769	76.53	1.250	0.352	−14.830
15	0.180	0.279	3.179	80.77	2.118	0.312	−21.473
20	0.196	0.303	5.200	83.57	2.317	0.328	−23.014

technique using dioxan as a medium. The effect of weight percent of bismuth oxide content on porosity factor is shown in Fig. 6. It is evident that the percentage porosity factor decreases as function of bismuth oxide content in sintered YZ at 1200 °C, 3 h.

The effectiveness of bismuth oxide addition as sintering aid is also evident from the SEM fractograph of the sintered specimens as shown in Fig. 7(a–e). A progressive change in microstructure with bismuth oxide is clearly visible. Fig. 7(a) shows no grains in the structure, but small grains and small pores are formed with addition of bismuth oxide. Fig. 7(c) shows dentritic structure. Even 20% bismuth oxide addition is not sufficient enough for complete densification of YZ.

The ionic conductivity of $Y_2Zr_2O_7$ with and without bismuth oxide addition was measured by a two-probe complex impedance analysis. The ionic conductivity (σ) has been measured in the temperature range of 500–800 °C. For all samples of YZ and mixed with 5–20% bismuth oxide, all were sintered at 1200 °C for 3 h. In general, the a.c. impedance of an ionic conductor measured by a two-probe method contains contributions from the bulk, grain boundaries and electrode/electrolyte interface, which can be reflected in a complex plane by three successive arcs, as shown in Fig. 8(a). The frequency increases from the right to the left across the plot. The arc at the high frequency end of the spectrum represents the bulk resistivity; the arc at the middle of the spectrum is a consequence of the grain boundary effect; the low-frequency arc is assigned to the electrode response. An idealized equivalent circuit for ceramic oxides corresponding to the impedance plot is shown in Fig. 8(b). In a practical case, however, not all these arcs can be observed, depending on the nature of the samples and testing conditions. Fig. 9 shows the impedance plots of samples with different bismuth contents measured at 500 °C in air. This figure clearly shows that the addition of bismuth oxide has a detrimental effect on grain boundary behaviour.

Fig. 10 represents the plot of logσ and 1/T for the sample without bismuth oxide. It was found that a straight line and the conductivity increase with increasing temperature. The activation energy of the plot is 7.841 kJ.

The effect of temperature on ionic conductivity for the samples with various percent of bismuth oxide is shown in

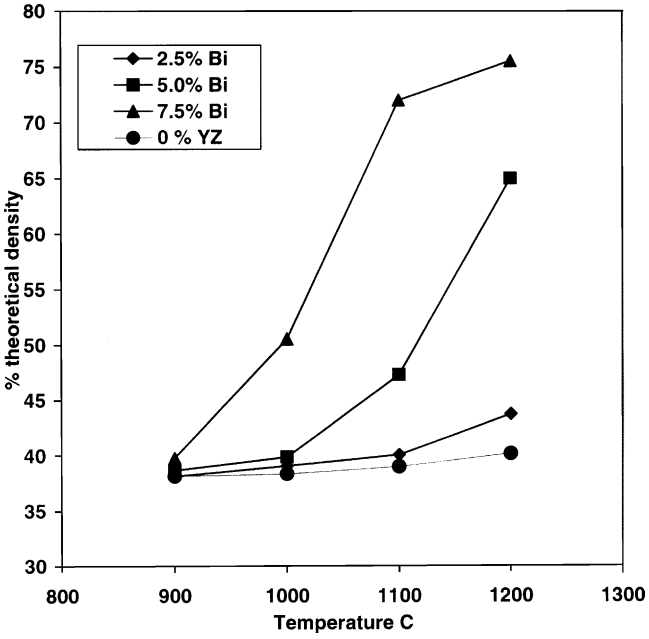

Fig. 5. The effect of temperature on percentage of theoretical density for yttrium zirconate pellet with and without bismuth oxide.

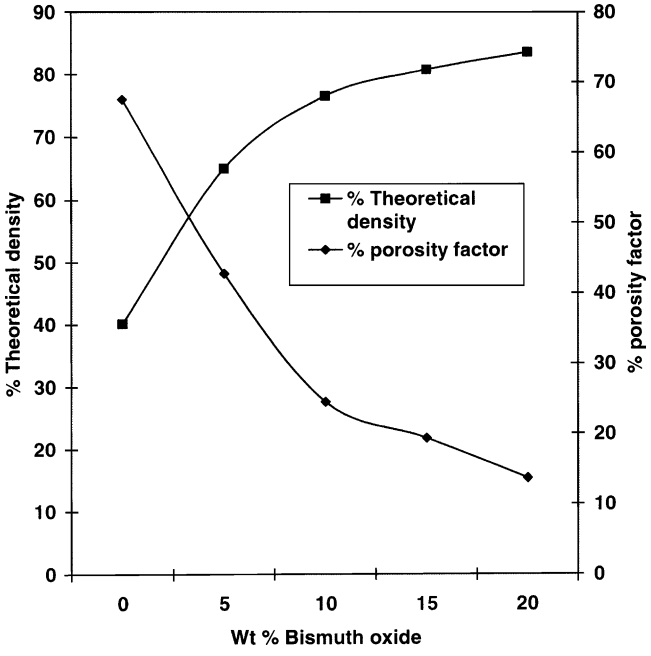

Fig. 6. The effect of bismuth oxide content on percentage theoretical density and on percentage of porosity factor for yttrium zirconate pellet with bismuth oxide.

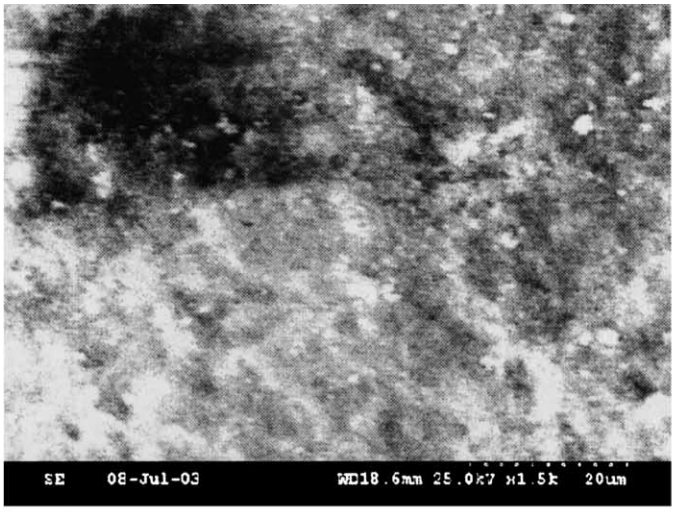

YZ 0%Bi

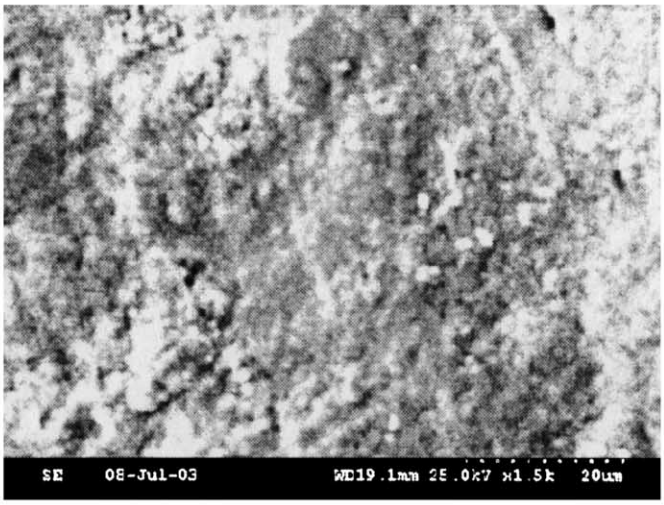

YZ15%Bi

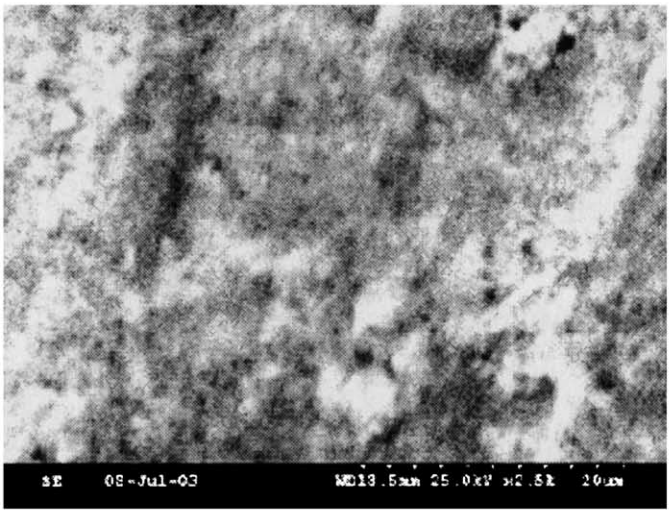

YZ 5%Bi

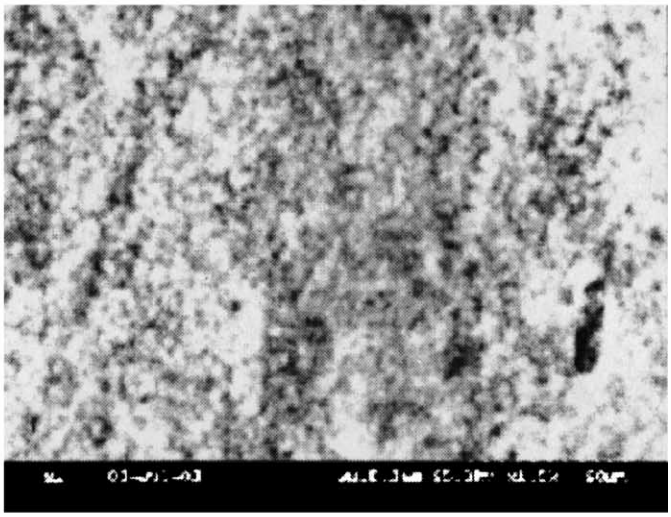

YZ20%Bi

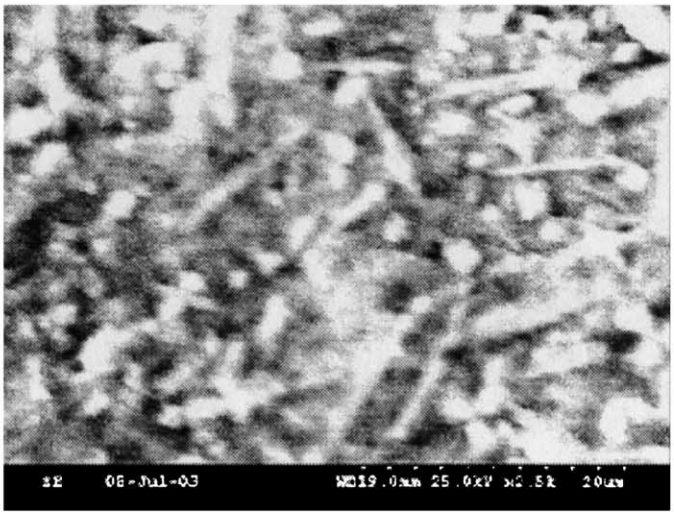

YZ10%Bi

Fig. 7. Microstructures for yttrium zirconate pellet with and without bismuth oxide.

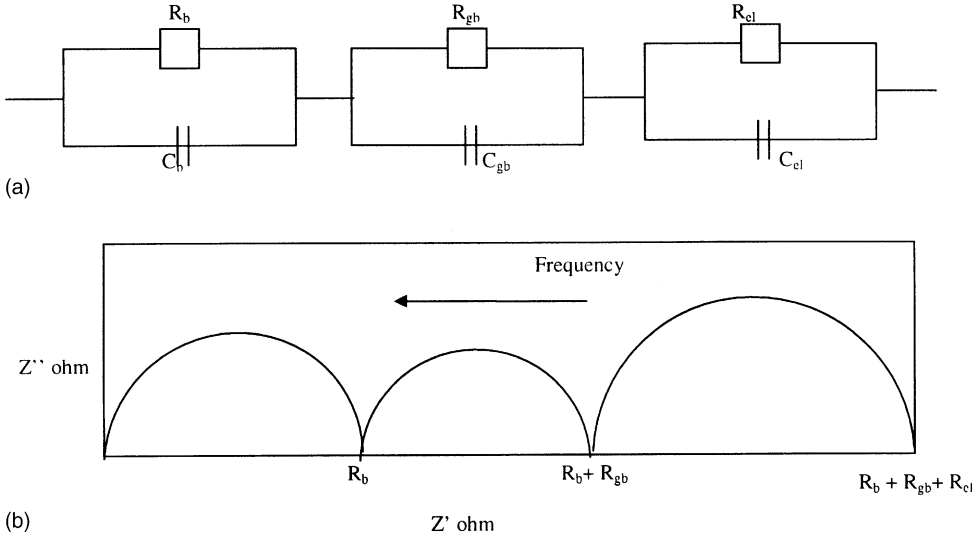

Fig. 8. An idealized equivalent circuit (b) and its corresponding impedance plot (a). C_b, R_b; C_{gb}, R_{gb}; and C_{el}, R_{el} represent resistance and capacitance for bulk, grain boundary, and electrode process, respectively.

Fig. 11. It is found that straight lines are obtained for the samples with 5, 10, 15 and 20%. The conductivity values and energy of activation are given in Table 1. From the graph, it is clear that at 500 °C, the conductivity value increases with increasing bismuth oxide content, and the conductivity value decreases with increasing bismuth oxide content at 800 °C [17]. The reason for the conductivity change was also identified from microstructures of those pellets. As expected, more and more dense microstructure is formed with increasing bismuth oxide content. Instead, the particles are grained with small pores, i.e., small pores increase with increasing bismuth oxide content; however, it has 83% of theoretical density at 20% bismuth oxide added YZ, which sintered at 1200 °C. As a result of experiment, the reduction of conductivity as increasing the bismuth oxide may be due to the formation of pores during sintering as shown in microstructure and compared with the unmixed YZ. Bismuth oxide mixed samples exhibit lower conductivity.

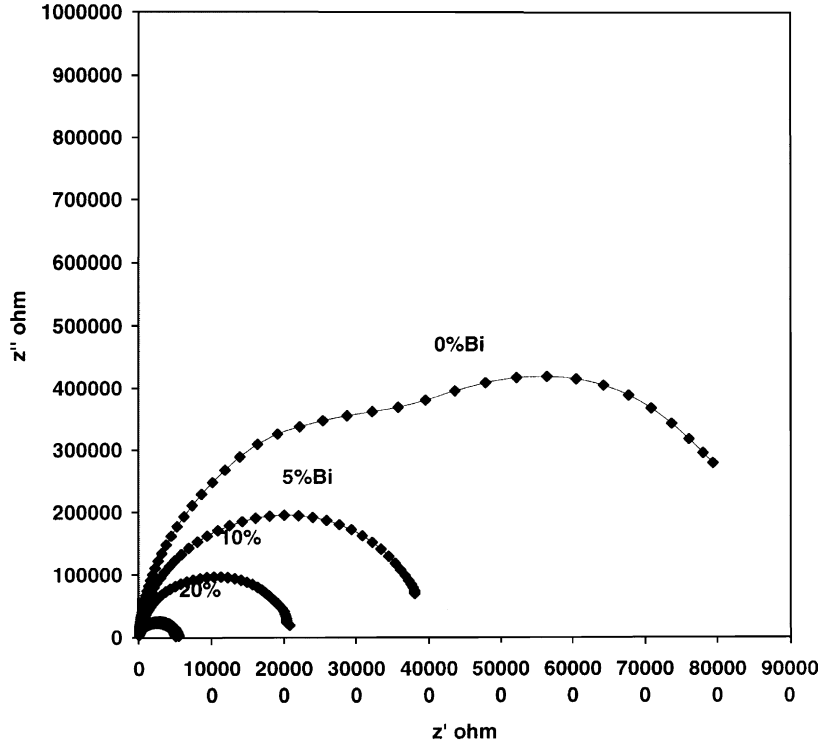

Fig. 9. The impedance plots of yttrium zirconate samples with different bismuth contents measured at 500 °C in air.

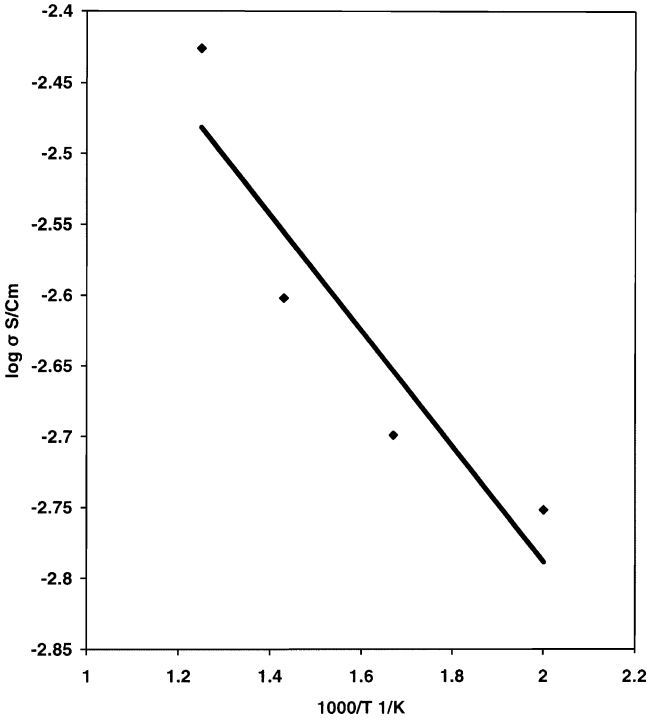

Fig. 10. Arrhenius plot for bulk conductivity of yttrium zirconate without bismuth oxide.

These results mainly from an enlarged grain boundary effect [18] in bismuth oxide mixed samples.

The effect of bismuth oxide on energy of activation and conductivity of pellets measured at 800 °C with and without bismuth oxide content are shown in Fig. 12. It reveals that the energy of activation decreases with increasing bismuth oxide content, but the conductivity of pellets measured at 800 °C initially decreases and the conductivity neither increases nor

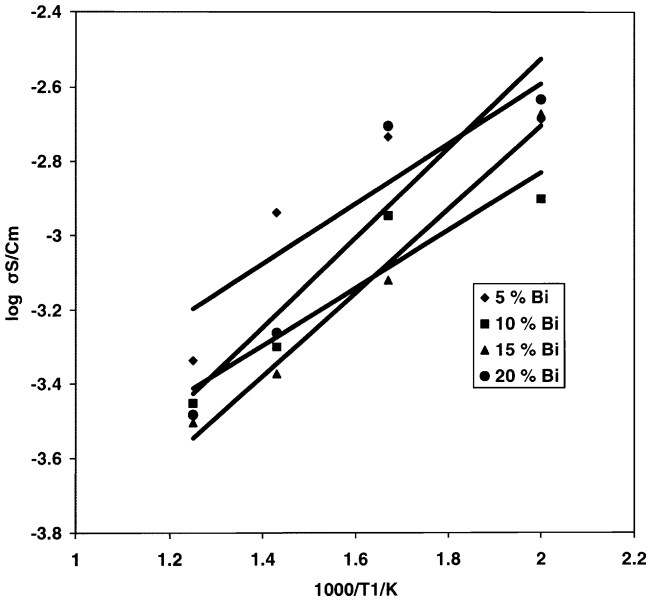

Fig. 11. Arrhenius plots for bulk conductivity of yttrium zirconate with bismuth oxide.

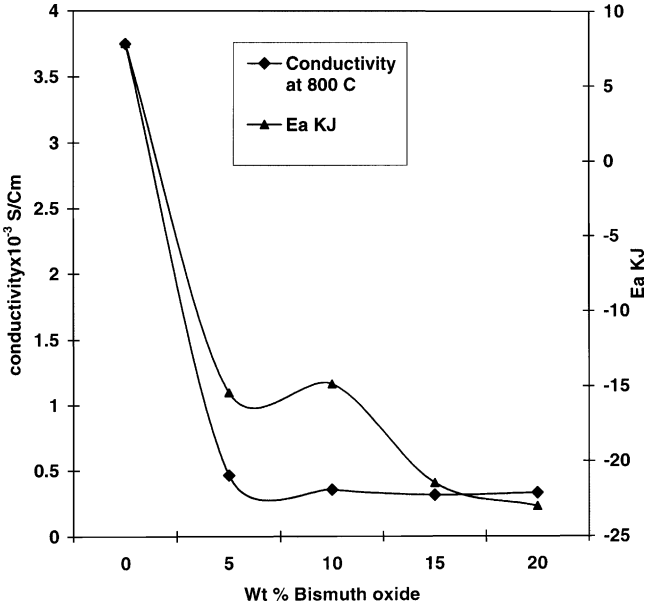

Fig. 12. The effect of bismuth oxide content on bulk conductivity measured at 800 °C and on energy of activation for yttrium zirconate pellets.

decreases with increasing bismuth oxide content. As a result, higher energy of activation seems to be responsible for the higher conductivity in yttrium zirconate without bismuth. Compared to yttrium zirconate with bismuth oxide, there is no marked difference in conductivity and energy of activation. The energy of activation is responsible not only for ion migration, but also for defect formation [16].

4. Conclusion

The glycine–nitrate combustion synthesis is a simple and convenient method to prepare yttrium zirconate powders. The thermal behaviour of YZ pellets is brought out from the steady state sintering experiments to draw useful information on the inter-dependence of percentage shrinkage in volume and the percentage densification factor with respect to the maximum attainable apparent percentage porosity for the first time. The bulk conductivity value of YZ is in the range of 10^{-3} S cm^{-1} at temperature range between 500 and 800 °C. Bismuth oxide was found to be an effective sintering aid. Even though it has increased the densification, it decreases the conductivity value of yttrium zirconate.

References

[1] N.Q. Minh, T. Takahashi, Science and Technology of Ceramic Fuel Cells, vol. 4, Elsevier Science, Amsterdam, 1995.
[2] Yamamoto Osamu, Electrochim. Acta 45 (2001) 2423.
[3] A. Samson Nesaraj, I. Arul Raj, R. Pattabiraman, Trans. SAEST 36 (2001) 89.
[4] K. Wiik, C.R. Schmidt, F. Scnem Shamsili, M.-A. Einarsrud, T. Grande, J. Am. Ceram. Soc. 82 (1999) 721.

[5] R. Doshi, V.L. Richards, J.D. Carter, X. Wang, M. Krumpelt, J. Electrochem. Soc. 146 (1999) 1273.
[6] A.J. Burggraaf, T. Van Dijk, M.J. Verkerk, Solid State Ionics 5 (1981) 519.
[7] M.P. Van Dijk, K.J. de Vries, A.J. Burggaaf, Solid State Ionics 9 (1983) 913.
[8] M.P. Van Dijk, A.J. Burggraaf, A.N. Cormack, C.R.A. Catlow, Solid State Ionics 17 (1985) 159.
[9] T. Moriga, A. Yoshiasa, F. Kanamaru, K. Koto, Solid State Ionics 31 (1989) 319.
[10] A.K. Shukla, J. Gopalakrishnan, Bull. Mater. Sci. 11 (1995) 109.
[11] P.K. Moon, H.L. Tuller, in: Subhash C. Singhal (Ed.), Proceedings of the First International Symposium on Solid Oxide Fuel Cells, The Electrochemical Society Inc., NJ, Proc, vol. 89–11, 1989, p. 30.
[12] S. Kramer, M. Spears, H.L. Tuller, in: S.C. Singhal, H. Iwahara (Eds.), Proceedings of the Third International Symposium on Solid Oxide Fuel Cells, The Electrochemical Society Inc., NJ, Proc, vol. 93-4, 1993, p. 119.
[13] N. Arul Dhas, K.C. Patil, J. Mater. Chem. 3 (1993) 1289.
[14] A.K. Bhattachaya, A. Hartridge, K.K. Mailick, J.L. Woodhead, J. Mater. Sci. 29 (1994) 6076–6078.
[15] D. Segal (Ed.), Chemistry of Solid State Materials: Chemical Synthesis of Advanced Ceramic Materials, Cambridge University Press, Cambridge, p. 23.
[16] V.V. Kharton, I.P. Marozau, N.P. Vyshatko, A.L. Shaula, A.P. Viskup, E.N. Naumovich, F.M.B. Marques, Mater. Res. Bull. 38 (2003) 773–782.
[17] M. Kumar, A. Samson Nesaraj, I. Arul Raj, R. Pattabiraman, International Conference on Ionic Devices, 28–30, Anna University, Chennai, India, 2003.
[18] T.S. Zhang, L.B. Kong, Z.Q. Zeng, H.T. Huang, P. Hing, Z.T. Xia, J. Kilner, J. Solid State Electrochem. 7 (2003) 348–354.